

## FABRICATION AND EVALUATION OF THE PHOTOCATALYTIC, ANTIBACTERIAL ACTIVITY OF Ag–TiO<sub>2</sub> THIN FILM

NU QUYNH TRANG TON<sup>1,†</sup>, THI NGOC TU LE<sup>1,2</sup>, DANG TRAI NGUYEN<sup>1</sup>,  
AND THI HANH THU VU<sup>1</sup>

<sup>1</sup>*University of Science, Vietnam National University, Ho Chi Minh City,  
227 Nguyen Van Cu, Ward 4, District 5, Ho Chi Minh City, Vietnam*

<sup>2</sup>*Dong Thap University,  
783 Pham Huu Lau Street, Ward 6, Cao Lanh City, Dong Thap Province, Vietnam*

<sup>†</sup>*E-mail: tonnuquynhtrang94@gmail.com*

*Received 30 December 2016*

*Accepted for publication 19 June 2017*

*Published 23 August 2017*

**Abstract.** *Ag–TiO<sub>2</sub> thin film was fabricated by the DC magnetron sputtering and photo-reduction methods. Characteristics of the film such as the surface morphology, crystal structure, and chemical composition were investigated by using the scanning electron microscope (SEM), X-ray diffractometry (XRD) and UV–Vis spectra. The photocatalytic activity of Ag–TiO<sub>2</sub> thin film was determined by the degradation of methylene blue (MB) solution under various irradiation conditions. The antibacterial property of Ag–TiO<sub>2</sub> thin film was conducted in *E. coli* bacteria. Results showed that the photocatalytic and antibacterial property of Ag–TiO<sub>2</sub> thin film are better than those of pure TiO<sub>2</sub> thin film in the visible region. Ag–TiO<sub>2</sub> thin film shows a great potential application in the antibacterial and environment field.*

**Keywords:** Ag–TiO<sub>2</sub>, thin film, DC magnetron sputtering, photocatalytic, antibacterial.

**Classification numbers:** 81.15.Cd; 81.16.Hc; 92.20.Jt.

### I. INTRODUCTION

TiO<sub>2</sub> has been widely studied as an effective photocatalytic for water treatment [1], air filter [2], antibacterial [3], self-cleaning materials [4], hydrogen generation by photocatalytic water splitting [5], etc. due to its low cost, nontoxic and environmentally friendly. However, TiO<sub>2</sub> has a wide band gap (3.2 eV) which only can be activated by UV region (only 5% of the solar radiation); besides that, the high recombination rate of electron–hole pairs would also decrease the

photocatalytic ability. There are many methods to the improvement of photocatalytic property of TiO<sub>2</sub> such as combining TiO<sub>2</sub> with other semiconductors (ZnO, CdS, ...) [6], metals (Ag, Pt, Cu, Fe, Ce, ...) [7] or non-metals (N, C, ...) [8]. Besides, depositing noble metals (Ag, Pt, Au, ...) is an effective solution for enhancing the photocatalytic ability of TiO<sub>2</sub>. Among noble-metals, Ag has attracted the attention of researchers because Ag has been found to be more effective due to it can trap the photo-generated electrons to reduce the recombination of electron-hole [9] and opens the ability to apply in the antibacterial field [10]. In addition, the Fermi energy level of noble metal is always lower than that of semiconductor photocatalysts and facilitates the photocatalytic activity in the visible light region. The charge separation and transfer of Ag and TiO<sub>2</sub> are displayed in Fig. 1. When TiO<sub>2</sub> absorbs photons of electromagnetic radiation with energy equal or greater than its band gap, an electron will jump from the valence band to the conduction band, and create electron (e<sup>-</sup>)-hole (h<sup>+</sup>) pairs. Before the photocatalytic reaction, the Ag<sup>+</sup> ion is adsorbed on the surface of TiO<sub>2</sub>, after the photocatalytic reaction the Ag<sup>+</sup> is reduced to Ag metal. Reactive oxygen species such as the hydroxyl radical (<sup>•</sup>OH), the superoxide anion radical (O<sub>2</sub><sup>-•</sup>) and hydrogen peroxide (H<sub>2</sub>O<sub>2</sub>) are the dominant species contributing to the degradation of various organic pollutants and breaking down bacterial cell walls.

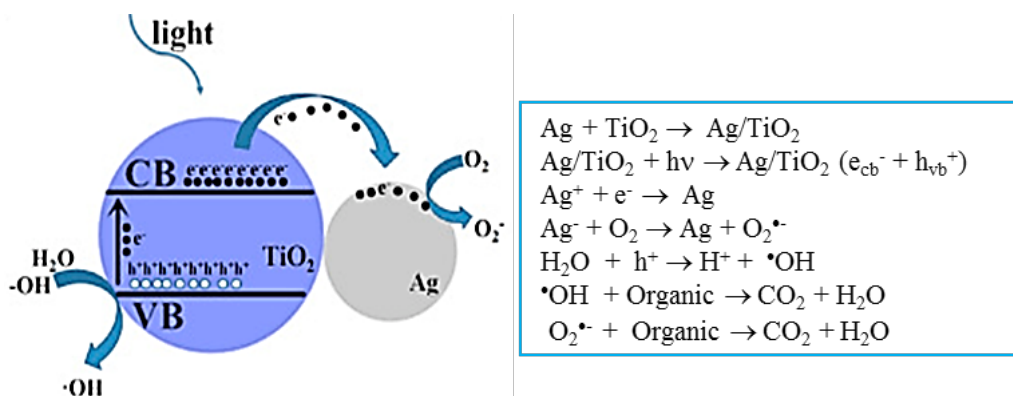


**Fig. 1.** Schematic diagram of the charge separation and transfer of Ag-TiO<sub>2</sub> structure [11].

The previous studies have been focused on the photocatalytic properties and the antibacterial ability of Ag-TiO<sub>2</sub> structures. Prakash Swarnakar *et al.* reported that silver-coated TiO<sub>2</sub> films could enhance MO degradation in sunlight and increase the rate 18% over the TiO<sub>2</sub> films under natural light. They indicated that the adsorption of Ag<sup>+</sup> significantly reduced the TiO<sub>2</sub> band gap in the visible region thus leading to the enhanced photocatalytic properties [12]. Ramacharyulu *et al.* also reported that Ag-TiO<sub>2</sub> film enhanced the rate of photocatalytic degradation of MB when compared to TiO<sub>2</sub> film due to the trapping the charge carriers of silver nanoparticles [13]. Selim Demirci *et al.* observed that Ag-doped TiO<sub>2</sub> films had better photocatalytic activity than un-doped TiO<sub>2</sub> film and 0.7% was an optimal dopant concentration exhibiting maximum photocatalytic activity. These results were explained by space charge creation and the rate of charge carrier recombination due to the presence of metallic Ag on TiO<sub>2</sub>, narrowing the band gap of the TiO<sub>2</sub> film [14]. Sornsanit K. *et al.* reported the Ag-TiO<sub>2</sub> composited films showed good optical

and high antibacterial activity at eliminating the *E. coli* bacteria after 20 minutes under UV irradiation [15]. Gupta et al. studied the antibacterial activity of TiO<sub>2</sub> and TiO<sub>2</sub> doped Ag nanoparticles on various strains (staphylococcus aureus, pseudomonas aeruginosin, and escherichia coli) under visible light irradiation [16]. Their studies indicated that the enhanced bactericidal activity in the dark and under UV illumination is due to the synergistic antibacterial effect of the photocatalytic reaction of the TiO<sub>2</sub> and the appearance of Ag nanoparticles on the surface. Which shows that TiO<sub>2</sub> surface modified with Ag is a research direction attracted a lot of interest because of improving the photocatalytic property and antibacterial ability of the material.

In this work, the TiO<sub>2</sub> thin film is fabricated by the DC magnetron sputtering method and surface modified Ag nanoparticles by the photo-reduction method. The morphology, crystalline phase and absorbance spectroscopy of the Ag-TiO<sub>2</sub> thin film are investigated by various characterization techniques (SEM, XRD, UV-Vis). In addition, the photocatalytic activity of the Ag-TiO<sub>2</sub> thin film is also evaluated using the degradation of methylene blue (MB) aqueous solution at  $\lambda = 664.6$  nm under various irradiation conditions. The antibacterial experiment was conducted on the *E. coli* bacteria by bacterial counting method.

## II. MATERIALS AND METHODS

### II.1. Materials

Materials used for the synthesis of pure TiO<sub>2</sub> thin film and Ag-TiO<sub>2</sub> thin film were Ti target (99.9%), silver nitrate (AgNO<sub>3</sub> EMSURE, Merck, Germany), distilled water and methylene blue (MB, Merck, Germany).

### II.2. Synthesis of Ag-TiO<sub>2</sub>

The TiO<sub>2</sub> thin film is fabricated on soda-lime glass (Marienfeld, Germany 900) by DC magnetron sputtering method. The soda-lime glass was cleaned with acetone, alcohol, and then surface treated by plasma discharge in  $4.22 \times 10^{-3}$  torr vacuum before thin film deposition. A plate with 7.6 cm in diameter made from the pure (99.9%) Ti was used for the target. Before sputtering, the Ti target was pre-sputtered for about 5 minutes with a shutter covering the substrate. TiO<sub>2</sub> thin film was deposited at the power of 100 W in 240 min, and the argon-oxygen flow rate ratio of Ar:O<sub>2</sub> = 6 : 20. The TiO<sub>2</sub> thin film was modified with Ag nanoparticles by the photo-reduction method and conducted according to the diagram in Fig. 2.

### II.3. Characterization methods

The crystal structure, morphology, and absorbance spectroscopy of Ag-TiO<sub>2</sub> thin film are characterized by X-ray diffraction (Bruker D8-ADVANCE), scanning electron microscope (SEM, FE-SEM Hitachi S-4800, and UV-Vis spectrophotometer (JASCO - V670), respectively. These measurements conducted at Nanotechnology Lab, SHTP labs.

The photo-catalytic activities of Ag-TiO<sub>2</sub> thin film are evaluated by the photo-degradation of methylene blue (MB) under different irradiation conditions: UV (Reptile UVB100-PT 2187, 25W), visible light (Compact Lamp-Philips, 25W). UV-Vis spectrophotometer (UV-2450; Shimadzu, Tokyo-Japan) is then used for monitoring the absorption of MB aqueous solution at a wavelength of 664.6 nm. The photocatalytic evaluation process performed at the Department of Applied Physics, Faculty of Physics & Engineering Physics, University of Science - VNUHCM. The antibacterial activity test is performed against *E. coli* (gram-negative and gram-positive) with

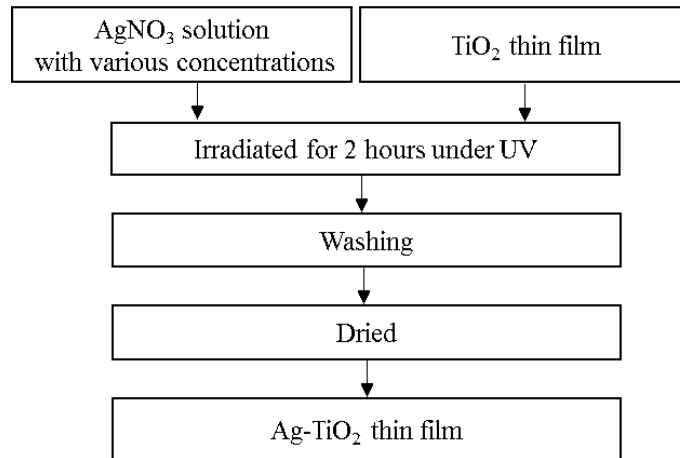


**Fig. 2.** The fabrication process of the Ag-TiO<sub>2</sub> thin film.

the initial bacterial cell concentration is about  $1 \times 10^5$  CFU/mL. The inactivation of *E. coli* on the Ag-TiO<sub>2</sub> thin film is compared with the pure TiO<sub>2</sub> thin film. To quantitatively evaluate the antibacterial activity of samples, 20  $\mu$ L of *E. coli* is added to each sample with the approximate surface area of 1 cm<sup>2</sup>. The surfaces with bacterial suspension are illuminated with UV-light and visible light in 60 and 120 minutes. Then 50  $\mu$ L of the resultant bacterial suspension and its 10<sup>3</sup>-fold dilutions are spread onto the nutrient agar plates. The number of surviving luminescent bacterial colonies (colony forming unit, CFU) is counted after incubation at 37 °C for 24 hours. Then, they are counted by manual counting method, it means that the primary trick in colony-counting is to count each colony dot on the surface of petri dish. To easily and correctly count colonies, we conduct to place the grid over the plate. Generally, we have to count at least 3 times, and only use plates containing smaller than 300 colonies to count to make correctly the number of colonies, then average them to get an average of living number of living colonies accurately. The disinfection efficiency (D%) is calculated by the following formula:

$$D(\%) = \frac{C_{control} - C_{photocatalytic.material}}{C_{control}} \times 100,$$

where,  $C_{control}$  is the number of surviving bacteria in the control dish,  $C_{photocatalytic.material}$  is the number of living bacteria of each disk containing photocatalytic material.

This experiment is conducted at Biochemical Lab, Faculty of Biology & Biotechnology, University of Science - VNUHCM.

### III. RESULTS AND DISCUSSION

#### III.1. The morphological and crystal structure characteristics of pure TiO<sub>2</sub> thin film and Ag-TiO<sub>2</sub> thin film

Figure 3 shows the surface morphology and the transmittance of the TiO<sub>2</sub> thin film. The surface of pure TiO<sub>2</sub> thin film shows the film roughness with 290 nm film thickness (Fig. 3a), the transmittance is about 85% (Fig. 3b). Calculating the porosity of the TiO<sub>2</sub> thin film based on

the expression of Clausius Mosstti indicates that its porosity is 0.80, and fits with the model of Thornton [17].

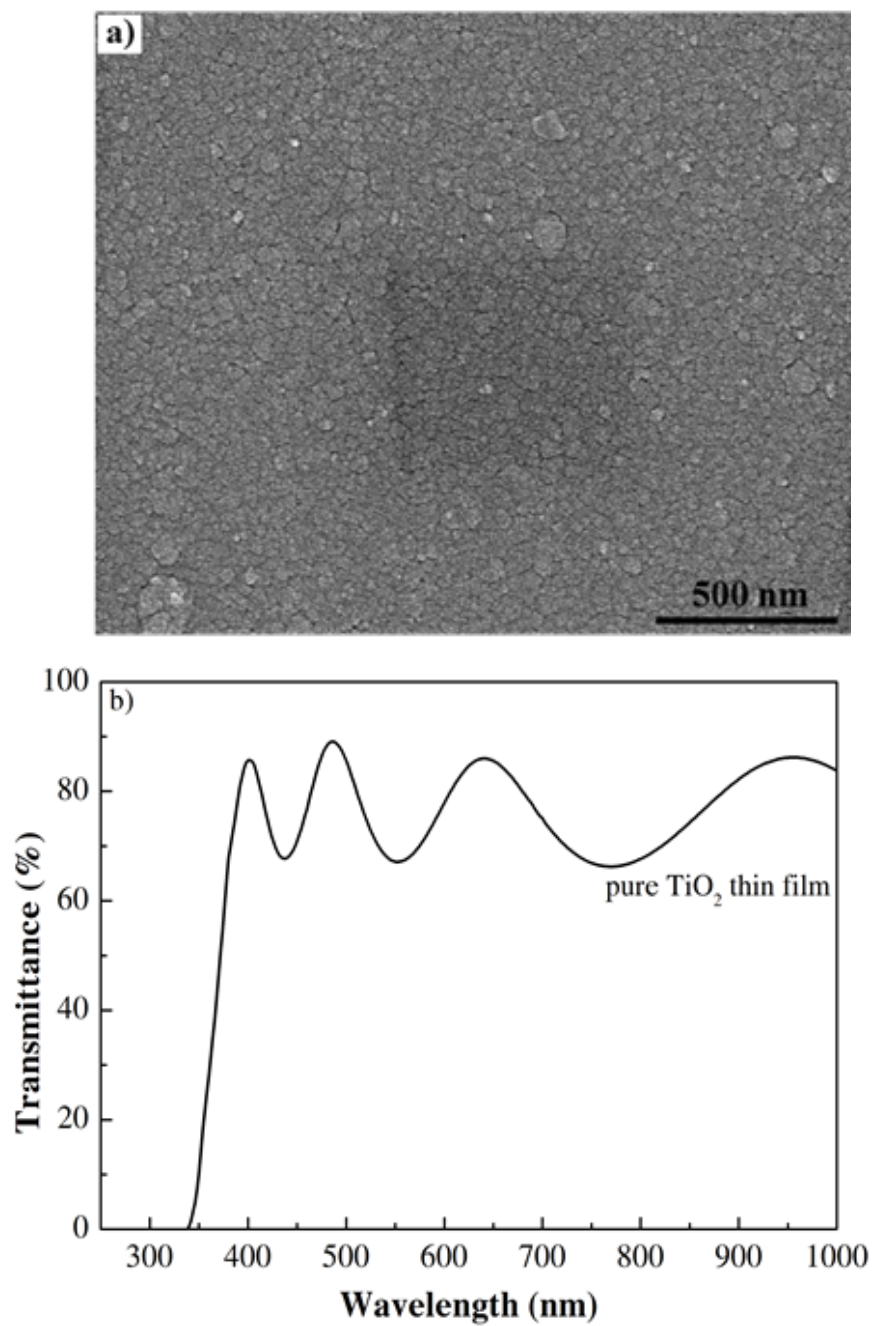


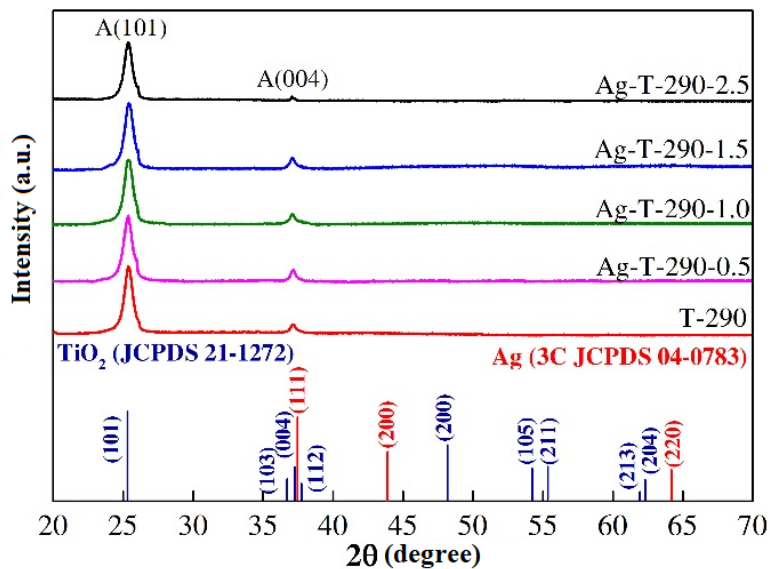
**Fig. 3.** The SEM images (a) and the transmittance pattern (b) of pure TiO<sub>2</sub> thin film.

TiO<sub>2</sub> surfaces modified with noble Ag nanoparticles via a photo-reduction method with the parameters preparation are presented in Table 1.

**Table 1.** The fabrication conditions of Ag-TiO<sub>2</sub> thin film with different AgNO<sub>3</sub>:TiO<sub>2</sub> ratio.

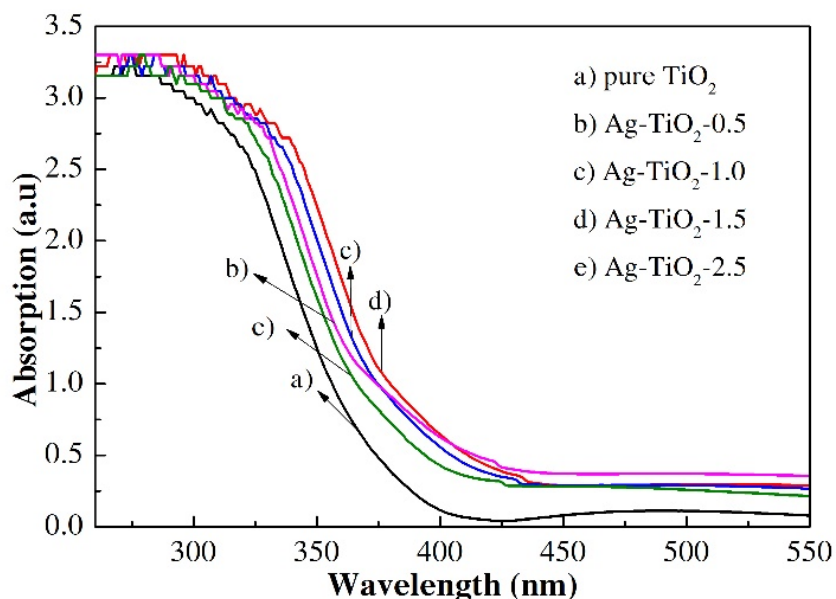
Samples	AgNO <sub>3</sub> : TiO <sub>2</sub> (wt)	The modification time (hours)
Pure TiO <sub>2</sub>	0.0:100	2
Ag-TiO <sub>2</sub> -0.5	0.5:100	2
Ag-TiO <sub>2</sub> -1.0	1.0:100	2
Ag-TiO <sub>2</sub> -1.5	1.5:100	2
Ag-TiO <sub>2</sub> -2.5	2.5:100	2

Figure 4 shows XRD patterns of pure TiO<sub>2</sub> and Ag-TiO<sub>2</sub>-1.0 thin films. The diffraction peak appears at  $2\theta = 25.08^\circ$  corresponding to A (101) peak along (001) crystal direction of TiO<sub>2</sub> anatase with the highest intensity and Ag peaks looking unclearly compare to others in this XRD result. However, the appearance of Ag in TiO<sub>2</sub> thin film leads to decrease their crystallinity or intensity of (101) peak.



**Fig. 4.** XRD pattern of pure TiO<sub>2</sub> film and Ag-TiO<sub>2</sub> with different AgNO<sub>3</sub>: TiO<sub>2</sub> ratio.

The UV-vis absorption spectra of the pure  $\text{TiO}_2$ , and  $\text{Ag-TiO}_2$  with different  $\text{AgNO}_3:\text{TiO}_2$  ratio is displayed in Fig. 5. Compared with the pure  $\text{TiO}_2$  thin film, the absorption spectrum of  $\text{Ag-TiO}_2$  samples show a single broad at the range of  $380\div 430$  nm, attributing to the charge-transfer from the valence band to the conduction band (Fig. 5). The optical bandgap energy ( $E_g$ ) of pure  $\text{TiO}_2$  and  $\text{Ag-TiO}_2$  are estimated by Kubelka-Munk equation ( $E_g = 1240.\lambda^{-1}$ ). The results show that the  $E_g$  of  $\text{Ag-TiO}_2$  samples ranged in  $3.15\div 3.2$  eV and narrower than that of pure  $\text{TiO}_2$  thin film, which indicate that the surface modification has expanded the absorption wavelength region of the pure  $\text{TiO}_2$  because of the surface plasmon resonance of noble metals on the surface of  $\text{TiO}_2$  [18].



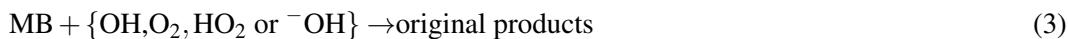
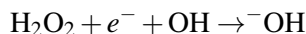
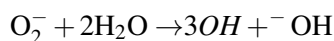
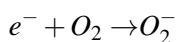
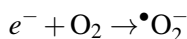
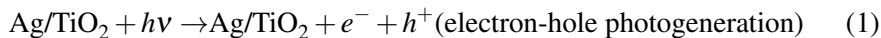
**Fig. 5.** UV-vis absorption spectra of (a) pure  $\text{TiO}_2$  and  $\text{Ag-TiO}_2$  with different  $\text{AgNO}_3:\text{TiO}_2$  ratio and (b) plots of  $[\alpha hv]^{1/2}$  versus photon energy ( $h\nu$ ) for samples given in (a).

### III.2. Photocatalytic activity and antibacterial ability of pure $\text{TiO}_2$ thin film and $\text{Ag-TiO}_2$ thin film

The photocatalytic ability of pure  $\text{TiO}_2$  thin film and  $\text{Ag-TiO}_2$  samples are evaluated by the degradation of MB in the presence of samples under the UV light and visible light (Fig. 6). The result shows that the degradation efficiency of MB solution of the pure  $\text{TiO}_2$  thin film,  $\text{Ag-TiO}_2-0.5$ ,  $\text{Ag-TiO}_2-1.0$ ,  $\text{Ag-TiO}_2-1.5$ , and  $\text{Ag-TiO}_2-2.5$  under UV light are in turn about 76%, 91%, 87%, 84%, and 82% within 90 min, respectively (Fig. 6a). This indicates that the UV light photocatalytic activity of the  $\text{Ag-TiO}_2$  thin film exhibits a higher photodegradation rate than pure  $\text{TiO}_2$  thin film samples. These results may be explained by following reasons:

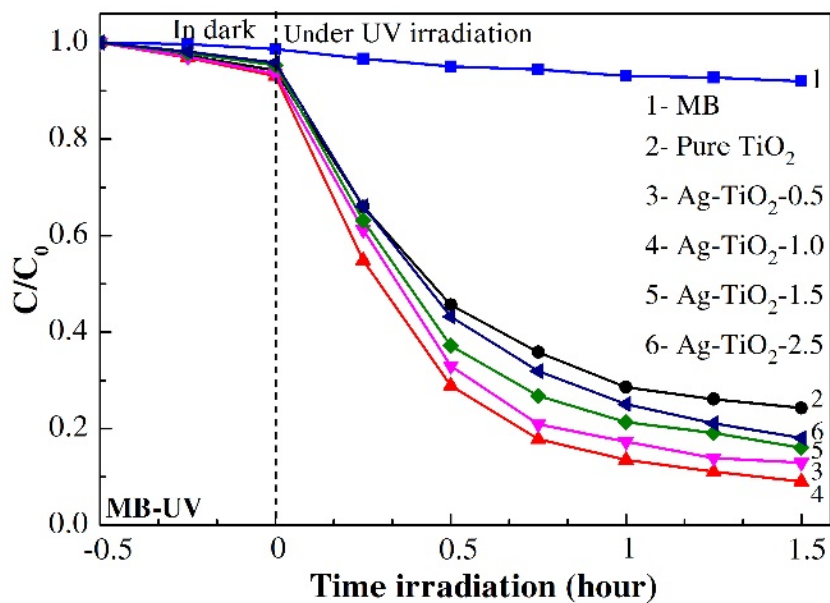
i) The enhanced photodegradation rate by  $\text{TiO}_2$  pure was attributed to by the reactive oxygen species (ROSs). While,  $\text{TiO}_2$  has been known as an UV absorbance material. So, when the  $\text{TiO}_2$  and  $\text{Ag-TiO}_2$  samples are irradiated under a suitable wavelength, the electron-hole pairs are

generated as indicated in Eq. (1). Then, they can react immediately with dye molecules (Eq. (2)) or with water and dissolved oxygen to produce free radical species and ROSs, such as OH, O<sub>2</sub><sup>-</sup>, HO<sub>2</sub> and H<sub>2</sub>O. They may produce oxidative stress and perform oxidation-reduction reactions leading to enhance dye molecules degradation (Eq. (3)). These above discussions are shown the following equations:

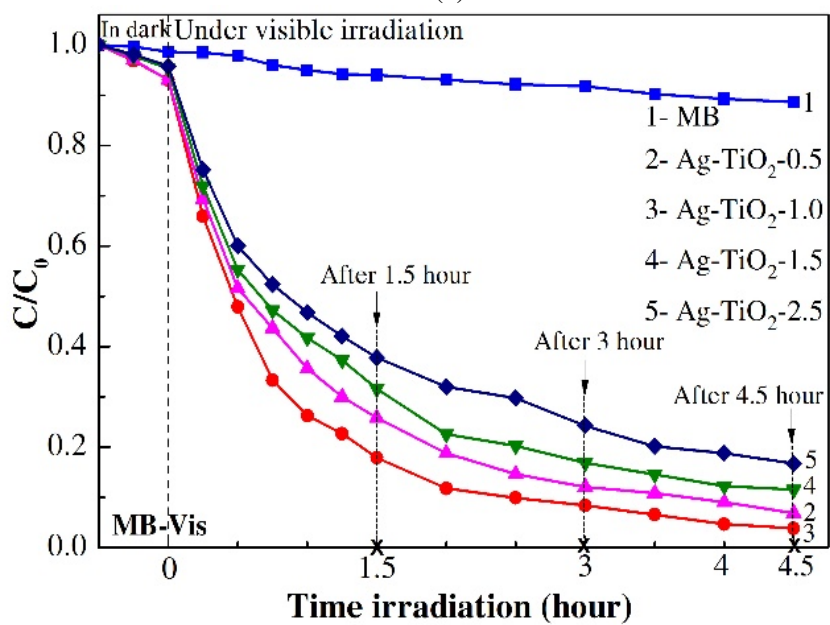


ii) The large specific surface area can enhance the UV light absorption leading to improve electron-hole photogeneration and improve photocatalytic efficiency. Whereas, the Ag contents were too much, it is possible that they would cover the TiO<sub>2</sub> surface and prevent light absorption, lead to decrease in photocatalytic efficiency. Additionally, the Schottky barrier formation established by the metal-semiconductor interaction. This plays a vital role in separating and inhibiting the rapid recombination of photogenerated electron-hole pairs. It is almost certain that the efficiency of photocatalytic activity can be significantly enhanced.

Under visible light, the degradation efficiency of MB solutions in Ag-TiO<sub>2</sub>-1.0 is 96% while Ag-TiO<sub>2</sub>-0.5, Ag-TiO<sub>2</sub>-1.5, and Ag-TiO<sub>2</sub>-2.5 turns in about 94%, 89%, and 84% (Fig. 6b). This means that the Ag-TiO<sub>2</sub> thin film samples show a higher photodegradation rate than the pure TiO<sub>2</sub> thin film in the visible irradiation, and the Ag-TiO<sub>2</sub>-1.0 thin film exhibits the best degradation efficiency of MB dye under the visible light. It may be explained by Ag deposition on the TiO<sub>2</sub> surface can act as electron-hole separation centers [19], and increase the rate of the electron-transfer process. According to the schematic diagram for the charge separation and transfer in Fig. 1, the electron transfer from the TiO<sub>2</sub> conduction band to metallic silver particles at the interface is thermodynamically possible because the Fermi level of TiO<sub>2</sub> is higher than that of silver metals [11]. This result in the formation of Schottky barrier at metal-semiconductor contact region, which limited the charge combination and enhanced the photocatalytic activity of the Ag-TiO<sub>2</sub> thin film. In addition, it has reported that the surface plasmon resonance (SPR) of noble metal and TiO<sub>2</sub> is excited by visible light, enhancing the surface electron excitation and electron-hole pairs separation [19]. All these led the Ag-TiO<sub>2</sub> thin film photocatalytic performance significantly improved. However, some previous studies reported that at the Ag contents above its optimum, the Ag particles could also act as recombination centers, which reduced the photocatalytic performance [20], and thus Ag content played a significant role in enhancing the photocatalytic activity of TiO<sub>2</sub>.



(a)

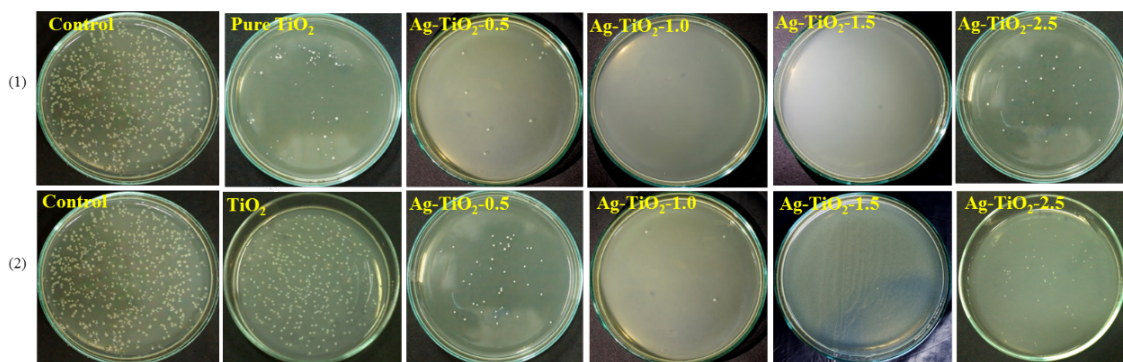


(b)

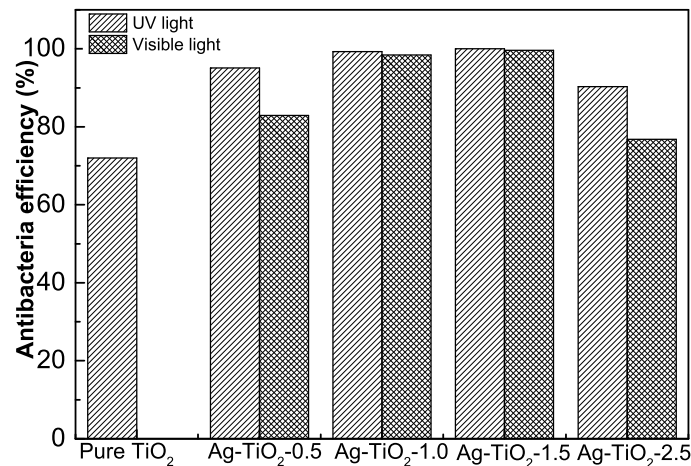
**Fig. 6.** Photocatalytic degradation of the aqueous MB under (a) UV irradiation, (b) visible irradiation with pure TiO<sub>2</sub> and Ag-TiO<sub>2</sub> samples.

Figure 7 (1) shows the antibacterial efficiency of the pure TiO<sub>2</sub> and Ag-TiO<sub>2</sub> thin films tested in UV irradiation for 60 min. It can be clearly seen that the pure TiO<sub>2</sub> thin film and Ag-TiO<sub>2</sub> samples have high antibacterial effect under UV irradiation. However, the pure Ag-TiO<sub>2</sub>

thin film that shows a higher antibacterial efficiency compared with the pure TiO<sub>2</sub> thin film. The disinfection efficiency of the pure TiO<sub>2</sub> thin film, Ag-TiO<sub>2</sub>-0.5, Ag-TiO<sub>2</sub>-1.0, Ag-TiO<sub>2</sub>-1.5, and Ag-TiO<sub>2</sub>-2.5 are about 72%, 95.1%, 99.3%, 100%, and 90.3%, respectively (Fig. 8). The best disinfection efficiency is 1-1.5.wt% of Ag content. The major cellular constituents such as proteins, lipids, polysaccharides, and nucleic acids, are organic compounds which can be attacked by ROSs. So they are the typical photocatalytic disinfection process. Under UV light, the ROSs not only produced by TiO<sub>2</sub> when UV absorbed but also by Ag nanoparticles. The generation of ROSs in bacterial cells causes cell death. The higher of ROSs generated, the higher of antibacterial efficacy.



**Fig. 7.** Photographs of *E. coli* bacteria grown on agar plate treated with: (1) Under UV irradiation for 60 min; (2) Under visible irradiation for 120 min.



**Fig. 8.** The antibacterial efficiency of *E. coli* in the liquid film on pure TiO<sub>2</sub> thin film, Ag-TiO<sub>2</sub> thin film with the various concentration of Ag under 60 minutes of UV and 120 minutes of visible irradiation.

The antibacterial efficiency of the pure TiO<sub>2</sub> and Ag-TiO<sub>2</sub> thin films test in the visible irradiation for 120 min is showed in Fig. 7 (2). The result indicates that the Ag deposited on

the TiO<sub>2</sub> thin film surface have the higher disinfection efficiency than pure TiO<sub>2</sub> thin film and the visible light antibacterial performance of Ag–TiO<sub>2</sub> thin film increases with an increasing in Ag concentration from 2.5÷10%. It shows clearly that the inhibition efficiency of Ag–TiO<sub>2</sub>–1.5 is 99.6% while Ag–TiO<sub>2</sub>–0.5, Ag–TiO<sub>2</sub>–1.0, and Ag–TiO<sub>2</sub>–2.5 thin film are about 82.9%, 98.4%, and 76.8%, respectively (Figure 8). The best disinfection efficiency is 1–1.5.wt% of Ag content. Those results may be explained by following reasons: i) the antibacterial activity of Ag nanoparticles is due to their ability of producing ROSs; ii) the formation of Schottky barrier between Ag–TiO<sub>2</sub> prevent the electron–hole pairs recombine rapidly, and the amount of reactive oxygen species (ROSs) is increased Thus, Ag deposition on TiO<sub>2</sub> thin film displays significant antibacterial effect in the visible light environment.

#### IV. CONCLUSIONS

In this work, the pure TiO<sub>2</sub> and Ag–TiO<sub>2</sub> thin film are fabricated by the DC magnetron sputtering method and photo-reduction process. The results show that Ag deposition on TiO<sub>2</sub> thin film surface effects the crystal structure, and the absorption of the Ag–TiO<sub>2</sub> thin film would be enhanced in the visible light region. The TiO<sub>2</sub> thin film was modified with Ag nanoparticles with a various Ag content showed an increase in the MB photodegradation under UV and visible irradiation as compared to the pure TiO<sub>2</sub> thin film. The inactivation of E. coli under UV and visible irradiation of pure TiO<sub>2</sub>, and Ag–TiO<sub>2</sub> thin film with different Ag concentration are compared. It is found that the photocatalytic property and antibacterial ability of Ag–TiO<sub>2</sub> thin film depend on Ag content and irradiation condition, in which, Ag–TiO<sub>2</sub>–1.5 sample exhibited the best antibacterial efficiency under UV and visible irradiation.

#### ACKNOWLEDGMENT

We gratefully thank Ho Chi Minh Department of Science and Technology support for this project with number 147/2016/HĐ-SKHCN.

#### REFERENCES

- [1] T. Bora and J. Dutta, *Journal of nanoscience and nanotechnology* **14** (2014) 613.
- [2] V. Puddu, H. Choi, D. D. Dionysiou and G. L. Puma, *Appl. Catal., B* **94** (2010) 211.
- [3] J. Ding, *Preparation of tio2 photocatalysis antibacterial ceramics*, Key Engineering Materials, vol. 575, Trans Tech Publ, 2014, pp. 302–305.
- [4] C. Garlisi, G. Scandura, A. Alabi, O. Aderemi and G. Palmisano, *J. Adv. Chem. Eng.* **5** (2015) e103.
- [5] J. Zhu and M. Zäch, *Curr. Opin. Colloid Interface Sci.* **14** (2009) 260.
- [6] M. Gholami, M. Shirzad-Siboni, M. Farzadkia and J.-K. Yang, *Desalin. Water Treat.* **57** (2016) 13632.
- [7] X. Yuan, W. Xu, F. Huang, D. Chen and Q. Wei, *Surf. Eng.* **33** (2017) 231.
- [8] V. Vaiano, O. Sacco, D. Sannino, P. Ciambelli, S. Longo, V. Venditto and G. Guerra, *J. Chem. Technol. Biotechnol.* **89** (2014) 1175.
- [9] R. S. Varma, N. Thorat, R. Fernandes, D. Kothari, N. Patel and A. Miotello, *Catal. Sci. Technol.* **6** (2016) 8428.
- [10] K. Ubonchonlakate, L. Sikong and F. Saito, *Procedia Engineering* **32** (2012) 656.
- [11] T. Wang, J. Wei, H. Shi, M. Zhou, Y. Zhang, Q. Chen and Z. Zhang, *Physica E Low Dimens. Syst. Nanostruct.* **86** (2017) 103.
- [12] P. Swarnakar, S. R. Kanel, D. Nepal, Y. Jiang, H. Jia, L. Kerr, M. N. Goltz, J. Levy and J. Rakovan, *Solar Energy* **88** (2013) 242.
- [13] P. Ramacharyulu, G. Prasad, A. Srivastava et al., *RSC Advances* **5** (2015) 1309.

- [14] S. Demirci, T. Dikici, M. Yurddaskal, S. Gultekin, M. Toparli and E. Celik, *Appl. Surf. Sci.* **390** (2016) 591.
- [15] K. Sornsanit, M. Horprathum, C. Chananonawathorn, P. Eiamchai, S. Limwichean, K. Aiempakit and J. Kaewkhao, *Fabrication and characterization of antibacterial ag-tio2 thin films prepared by dc magnetron co-sputtering technique*, *Adv. Mat. Res.*, vol. 770, Trans Tech Publ, 2013, pp. 221–224.
- [16] K. Gupta, R. Singh, A. Pandey and A. Pandey, *Beilstein J. Nanotechnol.* **4** (2013) 345.
- [17] J. A. Thornton, *J. Vac. Sci. Technol.* **11** (1974) 666.
- [18] X. Zhou, G. Liu, J. Yu and W. Fan, *J. Mater. Chem.* **22** (2012) 21337.
- [19] B. Xin, Z. Ren, H. Hu, X. Zhang, C. Dong, K. Shi, L. Jing and H. Fu, *Appl. Surf. Sci.* **252** (2005) 2050.
- [20] M. Harikishore, M. Sandhyarani, K. Venkateswarlu, T. Nellaippan and N. Rameshbabu, *Procedia Materials Science* **6** (2014) 557.